Mon. Not. R. Astron. Soc. **000**, 1–4 (0000) Printed 4 August 2014 (MN LATEX style file v2.2)

QSO mock catalogs v1.0

Martin White

4 August 2014

ABSTRACT

We present a mock quasar catalog (`v1.0`) designed to fit the observed luminosity function and clustering of QSOs over a wide range of redshifts. The goal was to produce "boxes of QSOs" at different redshifts which can then be sampled and projected into an observed catalog while serving as 'truth' for tests. Each 'box of QSOs' contains magnitudes, positions and velocities for mock QSOs brighter than $M_i(z = 2) = -22$. This document provides the details of how the quasar mock catalogs were created and presents some comparisons to observational data.

1 MOCK CATALOGS

This document describes some mock catalogs which can be used to develop the analysis pipeline and perform mission optimization for `DESI`. Here the focus is on a mock quasar catalog (`v1.0`) designed to fit the observed luminosity function and clustering of QSOs over a wide range of redshifts. The goal is to produce "boxes of QSOs" at different redshifts which can then be sampled and projected into an observed catalog while serving as 'truth' for tests.

The basis for the QSO mock catalogs are the catalogs of halos from the `Outer Rim` N-body simulation performed by the ANL group within the HACC framework. The `Outer Rim` simulation employed $10,240^3$ particles in a periodic box of $3\,h^{-1}$Gpc on a side. I have assumed a flat ΛCDM model with $\Omega_m = 0.265$ and $h = 0.71$ throughout (see Table 1). Friends-of-friends halo catalogs were generated at a range of outputs, and I have used these as the basis for "boxes of quasars" which match published luminosity functions and clustering at selected redshifts.

To generate QSOs from the halo catalog I used the model of Conroy & White (2013) in its simplest form. The major simplification was that I ignored any QSOs which are hosted by satellite galaxies. This is a good approximation at high z, but becomes less valid below $z \approx 1$. Even at low z, however, the simplified model should be adequate for our purposes[1] (the number of satellite-hosted QSOs is always small, although not completely negligible at low z). In addition, I switched from using the SM-HM relation of Behroozi, Conroy & Wechsler (2010) to Moster et al. (2013), which is a more recent compilation. The Moster et al. (2013) SM-HM relation predicts a much lower central galaxy stellar mass in high mass halos at high z (~ 3) than the relation of Behroozi, Conroy & Wechsler (2010), and thus fewer very massive black holes at these redshifts.

As I first step I produced 'smooth' QLFs at closely spaced redshifts and over a wide range of magnitudes using the Conroy & White (2013) model (Fig. 1). These QLFs were produced by fitting the model of Conroy & White (2013) to the data for $0.5 < z < 6$ and fitting a smooth curve to the model parameters as a function of z. The model, with these interpolated parameters, was used to produce QLFs at the desired zs over a wide range of luminosities.

[1] At lower z we also lose faint QSOs due to the finite mass resolution of the simulation.

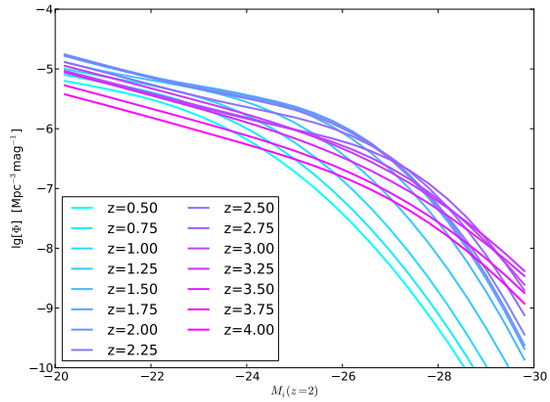

Figure 1. The model QLFs used as targets for the QSO model in the simulation box at each output. The smooth QLFs have been produced by fitting the model of Conroy & White (2013) to the data for $0.5 < z < 6$ and fitting a smooth curve to the model parameters as a function of z then using those models to produce QLFs at the desired zs over a wide range of luminosities.

Parameter	Value
$\omega_{\rm cdm}$	0.1109
$\omega_{\rm b}$	0.02258
n_s	0.963
h	0.71
w	-1.0
Ω_ν	0

Table 1. Parameters of the `Outer Rim` cosmological simulation. The box is 4225 Mpc or $3000\,h^{-1}$Mpc on a side and the particles are of uniform mass $m_p = 2.6{\times}10^9\,M_\odot = 1.9{\times}10^9\,h^{-1}M_\odot$. There are 100 time snapshots spaced evenly in $\ln a$ between $z = 10$ and $z = 0$, which leads to 34 outputs between $z = 1$ and 3.5. The halo catalogs give information for halos down to 20 particles, or $4 \times 10^{10}\,h^{-1}M_\odot$.

The model QLFs were used as targets to train the parameters of the QSO model in the simulation box at each output.

For each output of the simulation I then chose the interpolated QLF closest in redshift to the output and used the Conroy & White (2013) model to generate, from the halo catalog, a 'box of

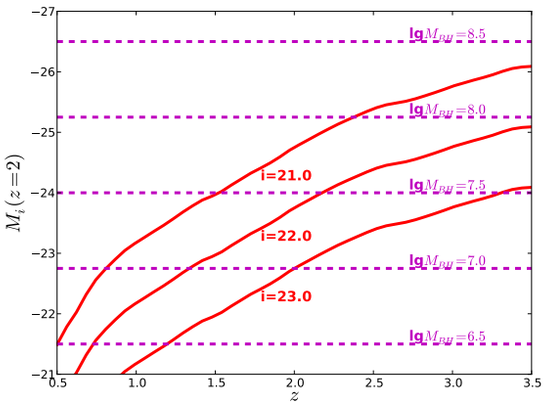

Figure 2. The luminosity-redshift plane. Horizontal lines show approximate values of the BH mass for a given absolute magnitude, while the solid red lines show the absolute magnitude corresponding to a given apparent i-magnitude limit assuming the k-correction of Ross et al. (2013) and the cosmology of the `Outer Rim` simulation.

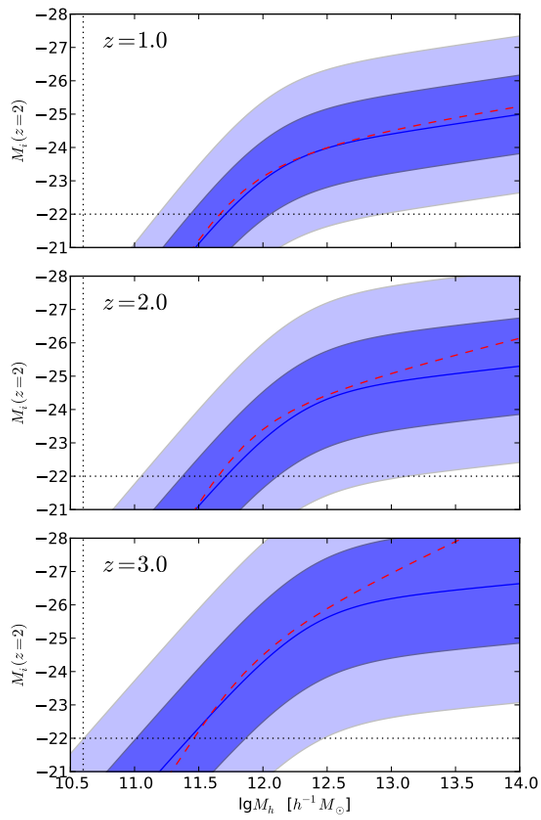

Figure 3. The mapping between halo mass and $M_i(z = 2)$ for the best-fit models at $z = 1$, 2 and 3. In each panel the solid line is the central value while the shaded bands show the approximate $1\,\sigma$ and $2\,\sigma$ scatter in $M_i(z = 2)$ at fixed halo mass. The dashed red line shows the central value assuming the SM-HM relation of Behroozi, Conroy & Wechsler (2010). The vertical and horizontal dotted lines show the mass limit of the halo catalog and the magnitude limit of the outputs (respectively).

3.75	3.50	3.25	3.00
2.75	2.50	2.25	2.00
1.75	1.50	1.25	1.00

Table 2. Redshifts at which we have produced a 'box of QSOs'.

QSOs' which most closely matches this QLF. Each QSO was assumed to be hosted by the central galaxy in the halo and inherited the halo's position and velocity. The catalog consists of these positions and velocities plus an absolute magnitude for each QSO. The magnitudes are stored as $M_i(z = 2)$, to conform to the convention most often used in SDSS and BOSS publications (though there are good reasons to modify this convention in the future: see Ross et al. (2013) for further discussion). To convert to M_{1450} one can use $M_{1450} \simeq M_i(z = 2) + 1.486$ and to convert to bolometric luminosity one can use $M_i(z = 2) = 72.5 - 2.5\mathrm{lg}L_{\mathrm{bol}}$ with the luminosity in Watts or $M_i(z = 2) = 90 - 2.5\mathrm{lg}L_{\mathrm{bol}}$ with the luminosity in erg s^{-1} (Shen et al. 2009). We kept only QSOs above $M_i(z = 2) = -22$, see Figs. 2 and 3.

Positions are stored in units of the box length (and run from $0 \cdots 1$ in each dimension) and velocities are stored as distance offsets to facilitate mapping to redshift space. If viewed along the z-axis, the redshift space coordinates of a QSO are $(x, y, z + v_z)$ [possibly periodically wrapped]. To convert to more conventional velocity units multiply each component of the velocity by aHL_{box}.

The typical magnitude of a QSO hosted in a halo of mass M_h for the best-fit models at $z = 1$, 2 and 3 are shown in Fig. 3. There is considerable scatter in observed luminosity at fixed halo mass, arising from scatter in the SM-HM relation, the BH-galaxy relation and the Eddington ratio. An estimate of the combined effects of this scatter are indicated by the shaded band.

2 COMPARISON TO OBSERVATIONS

Boxes of QSOs were generated at the list of redshifts given in Table 2 using the methods described above. To validate the catalogs and perform some cross-checks, we here present a comparison of the luminosity function and clustering of the mock QSOs to observations at some selected redshifts chosen to cover the range of interest of `DESI`.

Figure 4 shows the simulated QLF compared to observations. The simulated QLF was computed by simply binning the mock QSOs in bins of absolute luminosity and dividing by the volume of the box. The observations have all been converted to $M_i(z = 2)$ and references are given in the figure caption.

Figure 5 shows the projected clustering (w_p) compared to observations. The simulated w_p was computed by direct pair counting of the mock QSOs, integrating over $\pm 75\,h^{-1}$Mpc along the line-of-sight (taken to be parallel to the z-axis of the box). Note that the clustering in the lower redshift slices is slightly below the observational results, in part because of the neglect in the model of QSOs hosted by satellite galaxies in more massive halos. At higher redshifts the agreement is quite good, however.

3 QUASAR COLORS AND SELECTION

These boxes of QSOs need to be projected into the survey geometry and passed through the appropriate masks etc. In order to be 'observed' they need to be selected as targets and then have an efficiency of getting a good spectrum. A simple way to 'select' the

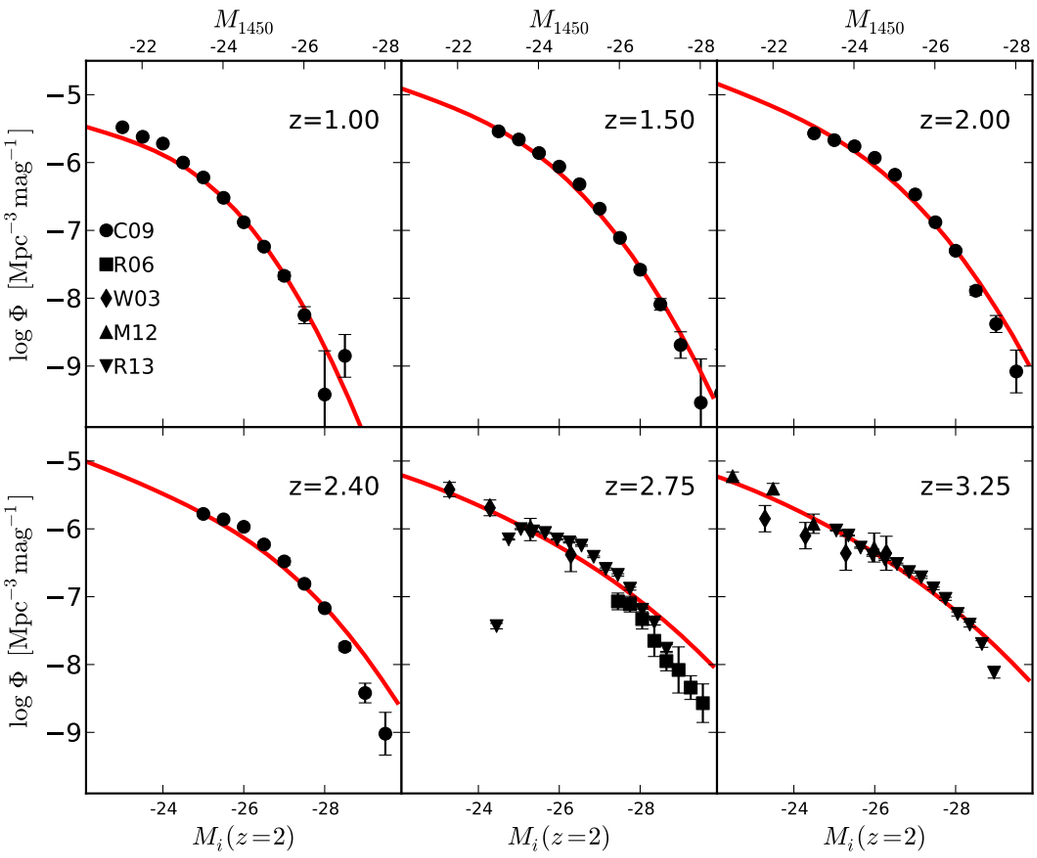

Figure 4. Comparison of the mock QLFs to observations at selected redshifts. In each panel the red line shows the histogram of the mock quasars in the simulation box, while the points with error bars show the data from Croom et al. (2009); Richards et al. (2006); Wolf et al. (2003); Masters et al. (2012); Ross et al. (2013), with all magnitudes converted to $M_i(z = 2)$ and M_{1450} as needed. For most data sets, the errors bars indicate only the statistical error. The simulations generally do a very good job of fitting the interpolated QLF, but for some redshifts (e.g. $z = 2.75$) the interpolated QLF has a hard time passing through all of the different data sets and picks a compromise solution.

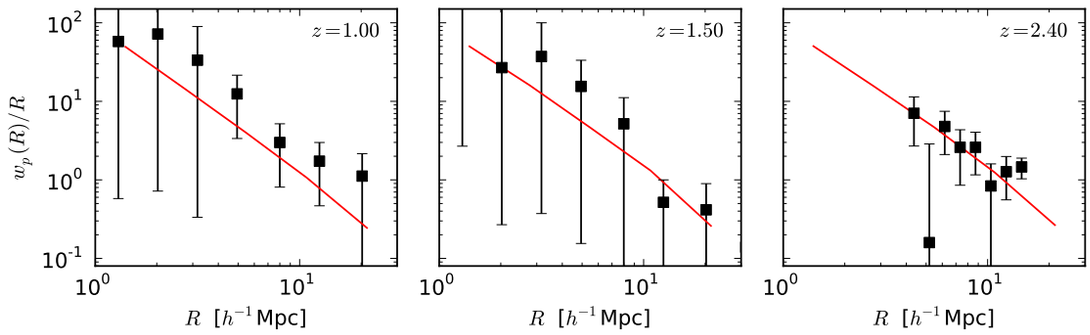

Figure 5. Comparison of the projected clustering of the mock QLFs to observations at selected redshifts. In each panel the red line shows the clustering of the mock quasars in the simulation box, while the points with error bars show the data from Ross et al. (2009); White et al. (2012). For the Ross et al. (2009) points the errors are based on Poisson errors, for the White et al. (2012) points the errors are determined from bootstrap resampling. Note that our simplification of the Conroy & White (2013) model leads to a slight underprediction of the clustering at low z.

targets would be to have a table of selection efficiency vs. luminosity and redshift and draw random numbers. Alternatively we could generate mock colors for the QSOs and apply some color cuts. To generate mock colors for the QSOs we need several inputs: the power-law continuum (with variable slopes?) and IR emission, possible contribution from the host galaxy at low z and L, Lyα and Lyman-limit system absorption and emission lines. Several partial or more complete models exist for each of these components (see for example the discussion in Ross et al. 2013 among many possibilities). We could also use composite spectra (e.g. from SDSS or BOSS) or synthetic spectra or objects from existing template libraries (e.g. Budavari et al. 2001).

REFERENCES

Behroozi, P., Conroy, C., Wechsler, R.H., 2010, ApJ, 717, 379
Budavari, T., Csabai, I., Szalay, A., et al., 2001, AJ, 122, 1163
Conroy, C., & White, M. 2013, ApJ, 762, 70
Croom, S. M., Richards, G. T., Shanks, T., et al. 2009, MNRAS, 399, 1755
Masters, D., Capak, P., Salvato, M., et al. 2012, ApJ, 755, 169
Moster, B., Naab, T., White S.D.M., 2013, MNRAS, 428, 3121
Richards, G. T., Strauss, M. A., Fan, X., et al. 2006, AJ, 131, 2766
Ross N. P., Shen Y., Strauss, M. A., et al. 2009, ApJ, 697, 1634
Ross, N. P., McGreer, I. D., White, M., et al. 2013, ApJ, 773, 14
Shen, Y., Strauss, M. A., Ross, N. P., et al. 2009, ApJ, 697, 1656
White, M., Myers, A. D., Ross, N. P., et al. 2012, MNRAS, 424, 933
Willott, C. J., Delorme, P., Reylé, C., et al. 2010, AJ, 139, 906
Wolf, C., Wisotzki, L., Borch, A., et al. 2003, AAP, 408, 499